SOCLIMPACT

Downscaling climate impacts and decarbonisation pathways in EU islands, and enhancing socioeconomic and non-market evaluation of Climate Change for Europe, for 2050 and beyond

Work Package 4:

Modelling Climate Impacts in 11 EU islands´ case studies for 2030- 2100

Deliverable 4.4c - Report on potential fire behaviour and exposure under climate change scenarios

Coordinated by CMCC (Valentina Bacciu and Liliana Del Giudice) with the participation of NOA (Maria Hatzaki) and reviewed by Salvador Suarez and Ghislain Dubois, according to the quality review internal process.

Revised version 20/01/2020

Type of deliverable: Other

Confidentiality level: PU

Version	Date	Author	N
v0	11/12/2019	Valentina Bacciu	1st outline sent to NOA
v1	22/12/2019	Maria Hatzaki	1st outline revised by NOA
v2	24/12/2019	Valentina Bacciu and Liliana Del Giudice	2nd draft of document reviewed internally
v3	31/12/2019	Valentina Bacciu	3rd draft of document reviewed internally
v4	20/01/2020	Valentina Bacciu	Version ready for Quality Review
v5	08/06/2020	Valentina Bacciu	Version ready for approval by the Project Officer

Table of Contents

1. Introduction

Fires have crucial role within Mediterranean ecosystems, with impacts both negative and positive on all biosphere components and with reverberations on different scales. Fire determines the landscape structure and plant composition, but it is also the cause of enormous economic and ecological damages, beside the loss of human life (Haas et al., 2015).

In the Mediterranean area, the occurrence of fires is mainly related to human activities (FAO, 2013) and varies considerably from year to year, suggesting a strong dependence on fire-weather conditions, such as drought and heat waves, as highlighted by Bedia et al. (2015) and Urbieta et al. (2015). However, during the past decades, fire frequency and fire extent have changed (Pausas and Fernández-Muñoz, 2012; Marques et al., 2011; Spano et al. 2014; Turco et al. 2016) as well as the burning patterns, especially in terms of expansion of the fire-prone areas (Arianoutsou et al., 2008; Fernandes et al., 2010; Koutsias et al., 2012) and lengthening of the fire seasons (e.g., Lavalle et al., 2009; Koutsias et al., 2015).

These changes have been linked to different transformations that have affected the entire Mediterranean basin concerning not only climate and weather, but also land use, socio-economic processes, and fire management (eg, Moreira et al., 2011; Viedma et al., 2015; Spano et al., 2014; Turco et al., 2016).

It is also widely recognized that wildfire risk and exposure are likely to be exacerbated by climate change (IPCC, 2014). In fact, a substantial increase in temperatures and drought conditions will likely alter the actual fire regime and may lead to an increase in fire hazard and risk. Indeed, extreme weather events, such as extended drought, heat waves and strong winds, facilitated the incidence and the behaviour of recent forest fires in Southern Europe, especially if supported by a general lack of forest management activities.

Within this context, understanding local climate change impacts and assessing vulnerabilities and risks are the first steps to provide information for identifying measures to adapt to climate change impacts and thus prepare effectively the landscape and the society for future risks imposed by climate change. Vulnerability and risk assessment under climate change encompasses a number of elements towards the efforts of expressing the complex interaction of different factors that determine the system proneness to be negatively affected.

Building on the fire weather index results of Deliverable 4.3 (*Atlases of newly developed hazard indexes and indicators*), which provided an evaluation of vulnerable areas with

respect to the potential of fire occurrence at the regional level under climate change by mapping the spatial and temporal distribution of fire danger, deliverable 4.4c applied high resolution fire spread and behaviour model within representative critical areas (Sardinia, Corsica, and Crete islands).

In particular, here we applied FlamMap model (Finney, 2006) which allows simulating thousands of fires and generating burn probability and intensity maps based on the minimum travel time (MTT) algorithm. The final aim of this deliverable was to

- estimate and evaluate potential fire characteristics and impacts (burn probability, expected burned areas, conditional flame length),
- and identify landscapes prone to large and severe fires, as well as the most relevant areas at high risk

under two RCP scenarios (2.6 and 8.5), two future scenarios (2026-2045 and 2081-2100), and using three RCM/GCM pairs, developed within the EURO-CORDEX initiative.

This approach and the results obtained can contribute to mapping fire regime changes due to climate change, and to support fire managers, decision and policy-makers to respond to the potential increase on fire vulnerability and risk.
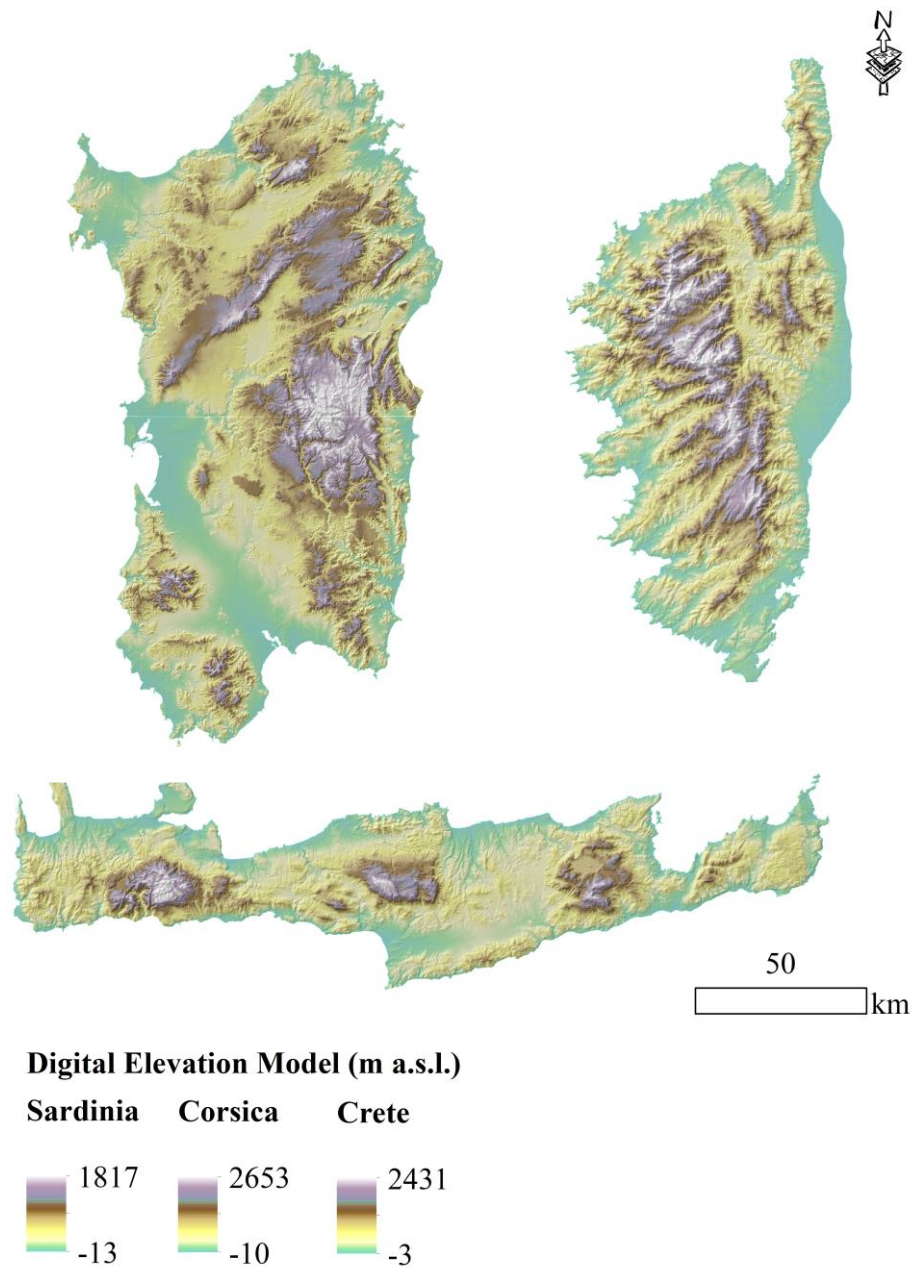
2. Material & Methods

2.2 Input Data for Fire Simulations

2.2.1 Topography and Fuels Data

FlamMap (Finney 2006) requires a gridded landscape file, composed of eight layers related to fuels and topography: elevation, slope, aspect, fuel models and canopy cover, canopy bulk density, canopy base height, and stand height. We assembled all input data at a 500-m resolution.

The topographic input data (elevation, slope and aspect) were derived from a 25-m digital elevation model of Sardinia, Corsica and Crete islands (https://land.copernicus.eu/imagery-in-situ/eu-dem) (Figure 1).

Figure 1 Digital Elevation Model of the three investigated islands

To define fuel type and canopy cover layers, we reclassified the Corine Land Cover map of 2018 (500 m resolution) following the methodology proposed by Salis et al., (2013). We obtained 13 fuel types, for which we associated standard or custom fuel models (Anderson 1982; Scott and Burgan 2005; Arca et al. 2009) from the original 44 Corine land cover categories present in the study area. The canopy fuel layers (canopy bulk

density, canopy base height, and stand height) were built using average values derived from the Italian Inventory of Forests and Forest Carbon Sinks (INFC, 2005).

Figure 2 Main vegetation types derived from the 2018 Corine Land Cover map of the three studied islands

2.2.3 Wind and Fuel Moisture for Fire Simulations

Wind speed and fuel moisture content data necessary for fire simulation were derived using 3-hourly climatic output from state-of-the-art RCM/GCM pairs, developed within the EURO-CORDEX initiative, for three periods [1986-2005 (baseline), 2046-2065 (near future) and 2081-2100 (distant future)]. The future period simulations of the models are based on the Representative Concentration Pathways (RCPs) 2.6 and 8.5. The selected RCM/GCM pairs are the following:

- **ICHEC-EC-EARTH/RCA4**
- **MPI-M-MPI-ESM-LR/RCA4**
- **MOHC-HadGEM2-ES/RCA4**

Wind speed frequency was estimated considering the fire season periods for each island and for each study period and the most recurring wind speed was used in the simulations.

We estimated dead and live fuel moisture using the Fine Fuel Moisture (FFMC) and Drought (DC) codes of the FWI system[1] as indicators, because have been demonstrated to be good estimators of dead and live surface fuel moisture in previous works (Lozano et al., 2017). FFMC, indeed, is a numerical ratings of the moisture content of litter and other fine fuels while DC represents the average moisture content of deep, compact organic layers. As FWI is based solely on meteorological variables, projected changes in temperature, precipitation, humidity and wind patterns under both RCP2.6 and RCP8.5 are reflected in the FWI patterns throughout the domain of study. In the framework of the project the FWI values for the fire season (May to October) are used as a climate hazard indicator under both RCP2.6 and RCP8.5 (Deliverable 4.3).

To estimate fuel moisture conditions, for each selected island and each period, we first calculated the frequency of different breakdown of fire weather codes, considering the fire season periods. DC and FFMC were classified based on values in Table 1 as "moderate," "moderate-dry", "dry," "very dry," and "extreme". Then specific fuel moisture conditions (Table 2) were associated to each classes, which were used in the simulations. Finally we calculated the percentage of days corresponding to the five fuel moisture categories.

---

[1] The FWI system provides numerical non-dimensional ratings of relative fire potential for a generalized fuel type (mature pine stands) based solely on weather observations. FWI is part of the Canadian Forest Fire Danger Rating System established in Canada since 1971 (van Wagner 1987). Furthermore, since 2007, FWI has been adopted at the EU level and used in a harmonized way throughout Europe by the European Forest Fire Information System (EFFIS) of the Copernicus Emergency Management Service (since 2015). **It is selected for exploring the mechanisms of fire danger change for the islands of interest in the framework of SOCLIMPACT Project**, as it has been proved to adequately perform for several locations, including the Mediterranean basin (e.g. Viegas et al. 1999; Dimitrakopoulos et al. 2011; Giannakopoulos et al. 2012; Bedia et al. 2013; Karali et al. 2014).

Table 1 – Classes of DC and FFMC and corresponding Fuel Moisture categories

Drought Code (DC)	Fine Fuel Moisture Code (FFMC)	Fuel Moisture classes
0 – 99	0 – 74	Moderate
100 – 175	75 – 84	Moderate-dry
176 – 249	85 – 88	Dry
250 – 299	89 – 91	Very dry
300 +	92 +	Extreme

Table 2 - Ranges of Dead and Live Fuel Moisture Values (in % of Dry Weight) Used as Simulation Input Data for the Different Vegetation Types

Moisture Category Label		Moderate	Moderate-dry	Dry	Very Dry	Extreme
Dead Fuel	1 h	14-16	11-13	9-11	7-9	5-7
	10 h	16-18	13-15	11-13	9-11	7-9
	100 h	18-20	15-17	13-15	11-13	9-11
Live Fuel	Shrubs	120-135	100-115	90-105	75-90	65-80
	Forests	120-135	100-115	90-105	75-90	65-80

2.3 Wildfire Simulations

The wildfire simulations were performed using the minimum travel time (MTT) fire spread algorithm of FlamMap. This technique calculates the fastest fire travel time along straight-line transects connecting nodes (cell corners) of the grid (Finney 2002, 2006). Surface fire spread is predicted by Rothermel's equation (1972) and crown fire initiation is evaluated according to Van Wagner model (1977) as implemented by Scott and Reinhardt (2001). We simulated 50,000 random ignitions for Sardinia and 20,000 for Corsica and Crete for each fuel moisture conditions.

Simulations were performed at 500 m resolution, in agreement with the inputs data, whith constant fuel moisture, and a burning period of 10 hours for each wildfire simulated and spot probability of 1%. Wind speed was fixed at 16 km h^{-1} and direction at 315° for

Sardinia and Corsica and 45° for Crete which reflected the most common conditions of the most extreme wildfire in the study areas.

FlamMap outputs were the burn probability, the conditional flame length, and the fire size. The burn probability (BP) is the spatially likelihood that a pixel will burn given a single fire in the study area. Another output of simulations is the Flame Length Probability (FLP) that represents the frequency distribution of flame lengths (FL) in 0.5-m classes for each pixel and was used to calculate the conditional flame length (CFL), which defines the weighted mean of the different FL generated from the multiple fires burning each pixel. Finally, the fire size output (FS) represents the extent of the fire for each ignition point in the simulations.

The obtained outputs were finally elaborated using Arcgis and weighting the percentage of days corresponding to the five fuel moisture categories described above for each study period, emission scenario, and climate model.

3. Results

3.1 Changes in DC and FFMC

As described above, we derived FFMC and DC codes for the baseline period 1986–2005 and for the two future periods, near future (2046–2065) and distant future (2081–2100), from the climate projections and we used these codes as indicators of fuel moisture.

The analysis of the baseline period (Table 3) highlighted for the DC that the frequency of "moderate" fuel moisture days for Sardinia was always about 50% considering icearth and mpi models, and about 42% for mohc model. The frequency of "extreme" fuel moisture days was about 25% for icearth and mpi models and about 30% for mohc model. The frequency of Corse value was always greater than 50% for "moderate" fuel moisture days considering icearth and mpi models and 44 % for mohc model, and about 20% for "extreme" for icearth and mpi models while 30% for mpi models. The results highlighted different frequency of fuel moisture conditions for Crete, where there are the highest value for "extreme" (about 60%) and the lowest value for "moderate" (about 20%) for all the three models.

Table 3 – Frequency of days (%) within DC Fuel Moisture categories during the baseline period for the three studied islands and the three climate models

	Sardinia			Corse			Crete		
	Icearth	Mohc	Mpi	Icearth	Mohc	Mpi	Icearth	Mohc	Mpi
Moderate	48	42	50	54	44	57	18	19	21
Moderate-dry	13	12	12	12	12	11	10	11	11
Dry	9	9	9	8	9	8	8	9	8
Very-dry	5	5	5	5	5	5	5	5	5
Extreme	26	31	24	21	30	19	60	56	55

Regarding the variation between the baseline period (1981–2010) and the near future period under the RCP 2.6, we observed

- Sardinia. An increase in the "moderate" class (10%) and a decrease in "extreme" value (5%) for the icearth model, while an increase (5%) in "extreme" class for the other models.
- Corse. The frequency of "moderate" days increased (5%) using the icearth model, while considering the other models we observed an increase in the frequency of "extreme" days (15% mohc, 6% mpi).
- Crete. The frequency of "moderate" days increased (25%) and of "extreme" days decreased (7%) using the icearth model; we observed an increase in the frequency of "extreme" days using the other models (10% mohc, 16% mpi).

Considering the variation between the baseline period (1981–2010) the distant future period under RCP 2.6, we observed

- Sardinia. The frequency of "moderate" and "extreme" days decreased (2%, 6%) using the icearth model; the frequency of "moderate" days increased (7%) and "extreme" days decreased (10%) using mohc model; and the frequency of "extreme" days increased (11%) using mpi model.
- Corse. Using the models icearth and mohc, the frequency of "moderate" days increased (1%, 11%) and "extreme" days decreased (6%, 13%), while for mpi model "extreme" value increased (27%) and "moderate" value decreased (7%).
- Crete. Using the icearth model the frequency of "extreme" days decreased (2%), while using the mohc and mpi models "extreme" value increased (7%).

Under RCP 8.5 the results highlighted that in general for Sardinia, Corsica and Crete the frequency of "extreme" days increased and the "moderate" days decreased for all three models, for both the near future and distant future (Figure 2). Considering Sardinia, the "extreme" days increased by 26%, 12% and 31% for icearth, mohc and mpi for Near Future and 56%, 42% and 74% for Distant Future. The "extreme" value in Corsica increased by 34% (icearth), 10% (moch) and 30% (mpi) for Near Future and 69% (icearth), 40% (moch) and 88% (mpi) for Distant Future. The "extreme" value in Crete increased by 7%, 11% and 15% for Near Future and 18%, 24% and 32% for Distant Future and for icearth, mohc and mpi models.
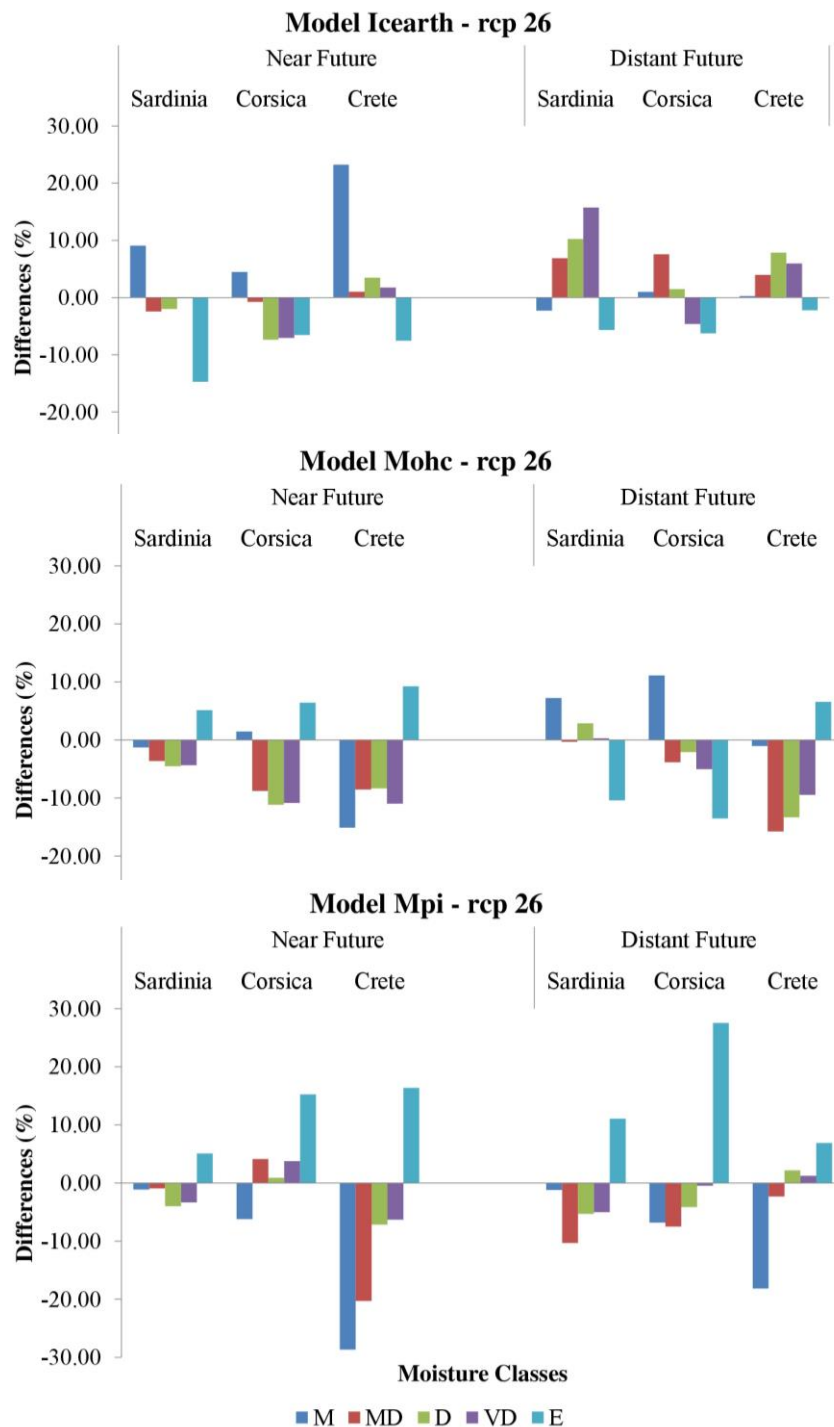
Figure 1 - Variation in DC from the baseline (1986–2005) to the Near Future (2045–2065) and Distant Future (2081–2100) for the three models under RCP 2.6
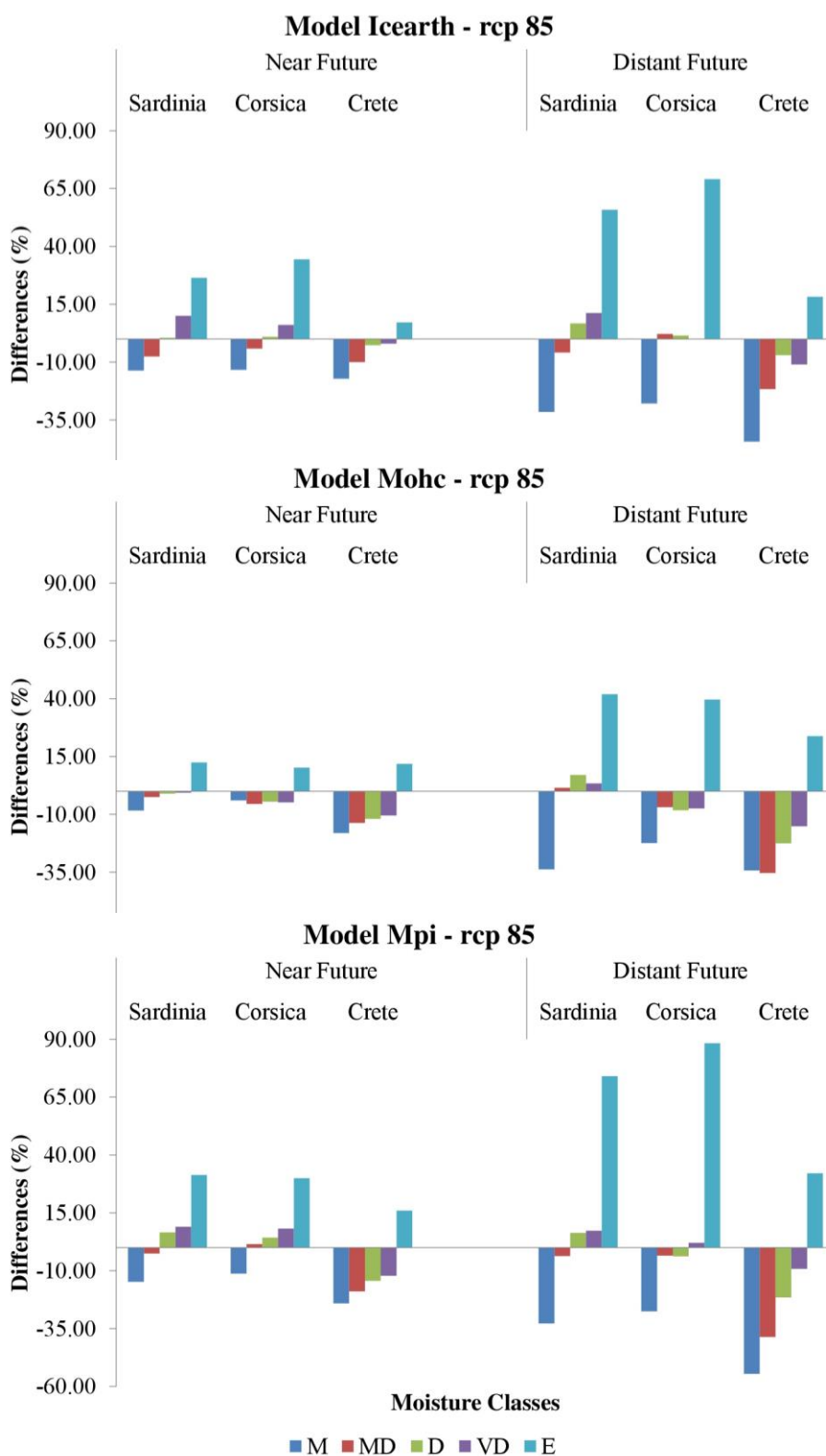
Figure 3 Variation in DC from the baseline (1986–2005) to the Near Future (2045–2065) and Distant Future (2081–2100) for the three models under RCP 8.5

The analysis of the baseline period of FFMC (Table 4) highlighted that the frequency of fuel moisture days was distributed more homogeneous than DC value for Sardinia and Corsica, while considering Crete there are the higher frequency for "moderate-dry" and "dry" value (about 30%).

Regarding the variation between the baseline period (1981–2010) and the Near Future period under RCP 2.6 we observed an increase in the frequency of "dry" (8%) and "extreme" (7%) days in Sardinia using the icearth model, while using mohc and mpi models there is a more marked increase in the frequency of "extreme" days (14 and 6%, respectively). This trend was similar in Corsica and Crete. In the Distant Future, the frequency of "extreme" days in Sardinia slightly decreased using the icearth and mohc models while increasing (13%) using the mpi model. Also in Corse and Crete this model showed the highest value of "extreme" days (21% and 27% respectively).

Table 4 - Frequency of days (%) within FFMC Fuel Moisture categories during the baseline period for the three studied islands and the three climate models

	Sardinia			Corse			Crete		
	Icearth	Mohc	Mpi	Icearth	Mohc	Mpi	Icearth	Mohc	Mpi
Moderate	25	22	26	30	25	30	11	12	12
Moderate-dry	25	22	24	25	22	25	31	28	27
Dry	18	19	19	21	22	21	31	31	34
Very-dry	13	15	13	15	18	15	15	16	16
Extreme	19	22	18	10	13	10	12	12	11

Under RCP 8.5, the results highlighted that in general for all three Islands the frequency of "extreme" days increased and the "moderate" value decreased for all three models and for Near Future and Distant Future.

In Sardinia, the differences in frequency of "moderate" days ranged from about 15% for Near Future to about 33% for Distant Future, while the differences in frequency of "extreme" days ranged from about 20% to 44-56%. Considering Corse, differences in "moderate" days ranged from about 10-17% for Near Future to about 30% for Distant Future, while the "extreme" days ranged from about 30-37% to 70-88%. Finally, in Crete, the change in frequency for "moderate" days ranged from about 20% for Near Future to about 40% for Distant Future, while the changes in "extreme" days ranged from about 24-34% to 50-66%.

Model Icearth - rcp 26

Model Mohc - rcp 26
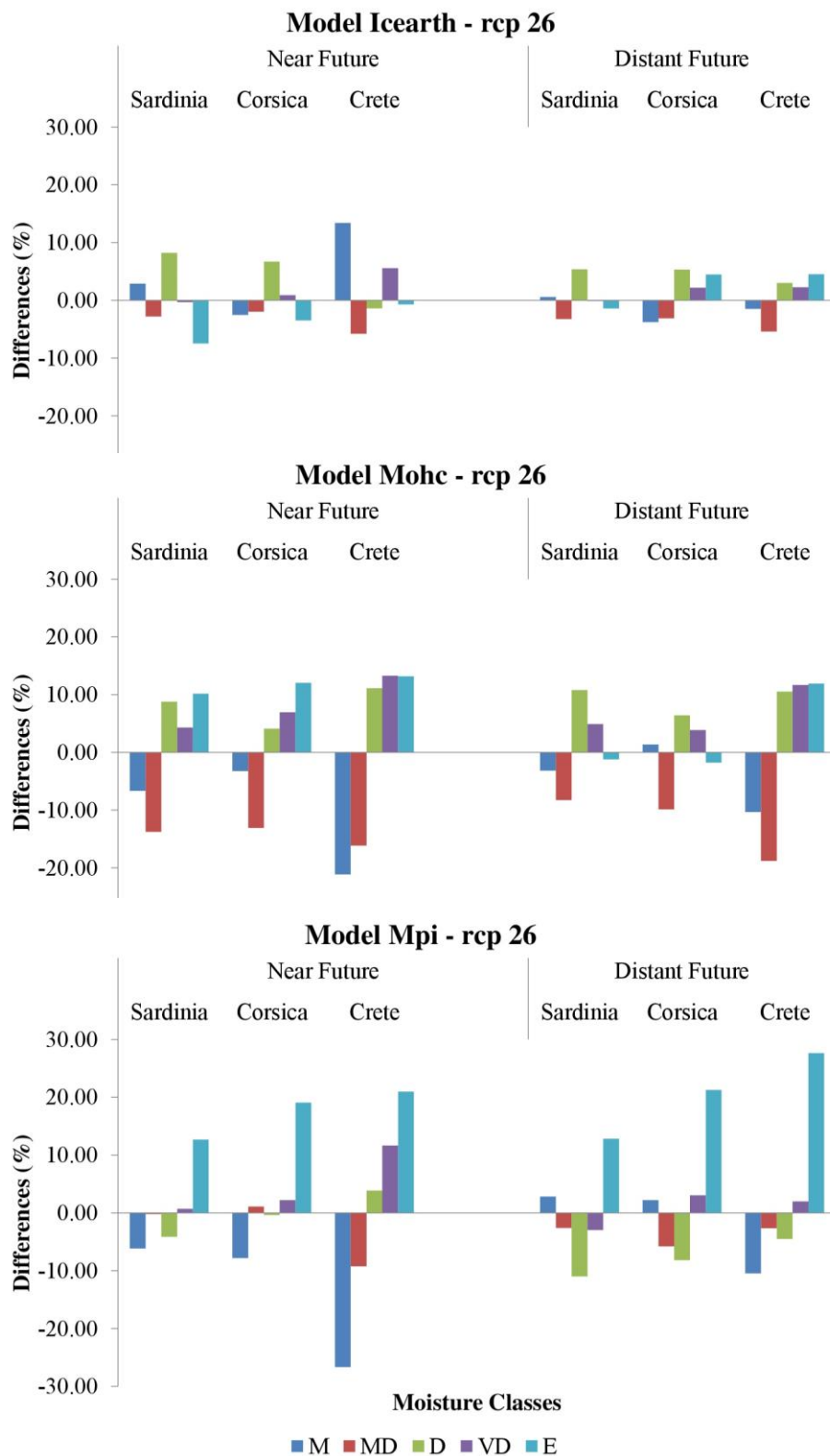
Model Mpi - rcp 26

Figure 4 Variation in FFMC from the baseline (1986–2005) to the Near Future (2045–2065) and Distant Future (2081–2100) for the three models under RCP 2.6.
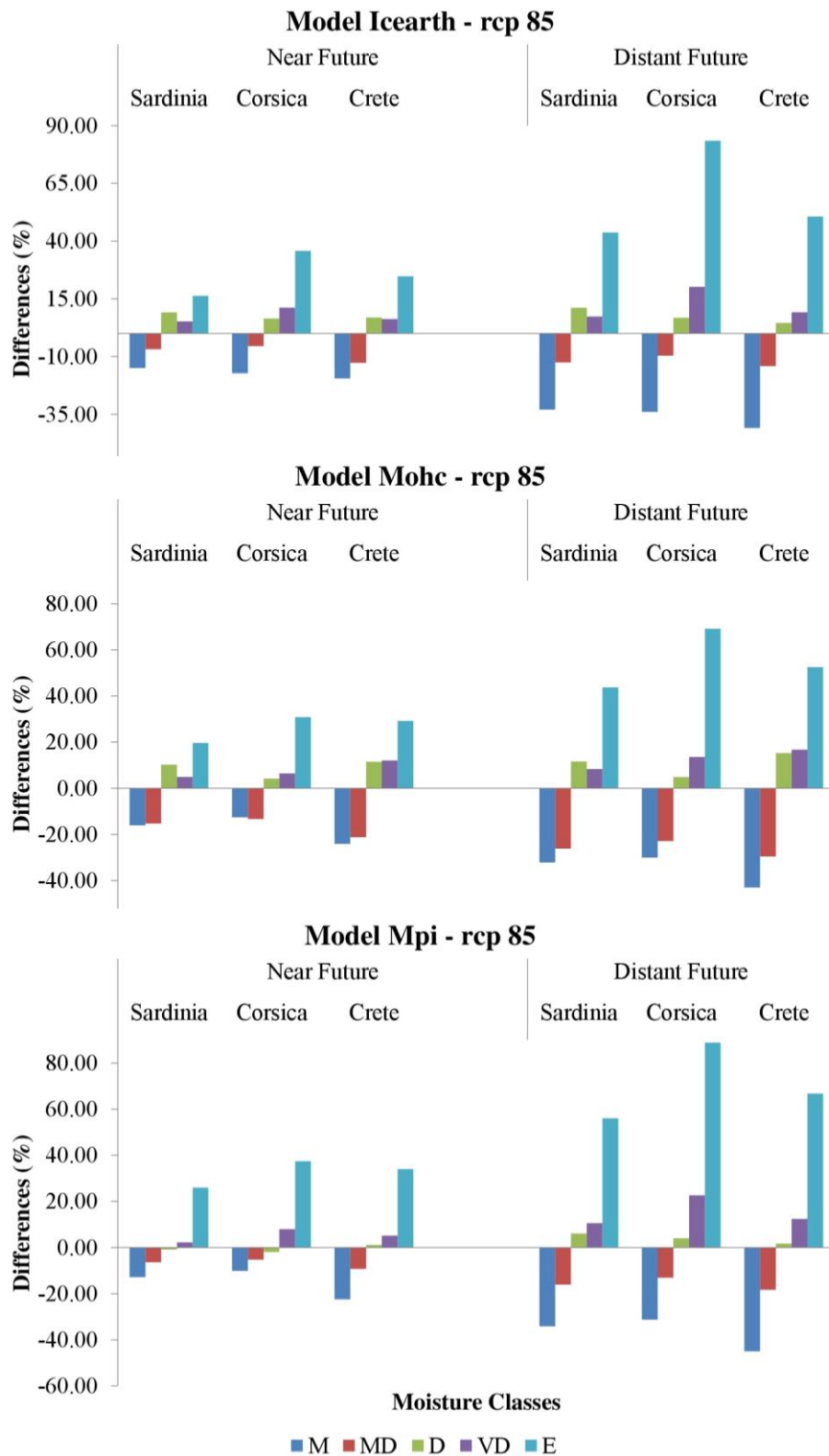
Figure 5 Variation in FFMC from the baseline (1986–2005) to the Near Future (2045–2065) and Distant Future (2081–2100) for the three models under RCP 8.5

3.2 Changes in Wildfire Exposure

From the outputs of FlamMap simulations, a set of fire exposure indicator maps (BP, CFL, FS) was derived for the different models, study periods and Islands at a spatial resolution of 500 m (see an example for Sardinia in Figure 6). In order to provide information on the most relevant areas at high risk, here we analysed the difference between the baseline period 1986-2005 and Near Future (2046-2065) and Distant Future (2081-2100) at the administrative level of NUTS3 (nomenclature of territorial units for statistics at level 3) (Figure 7). In addition, in Annex 1 the FS maps are provided to help in identifying landscapes prone to large and severe fires.
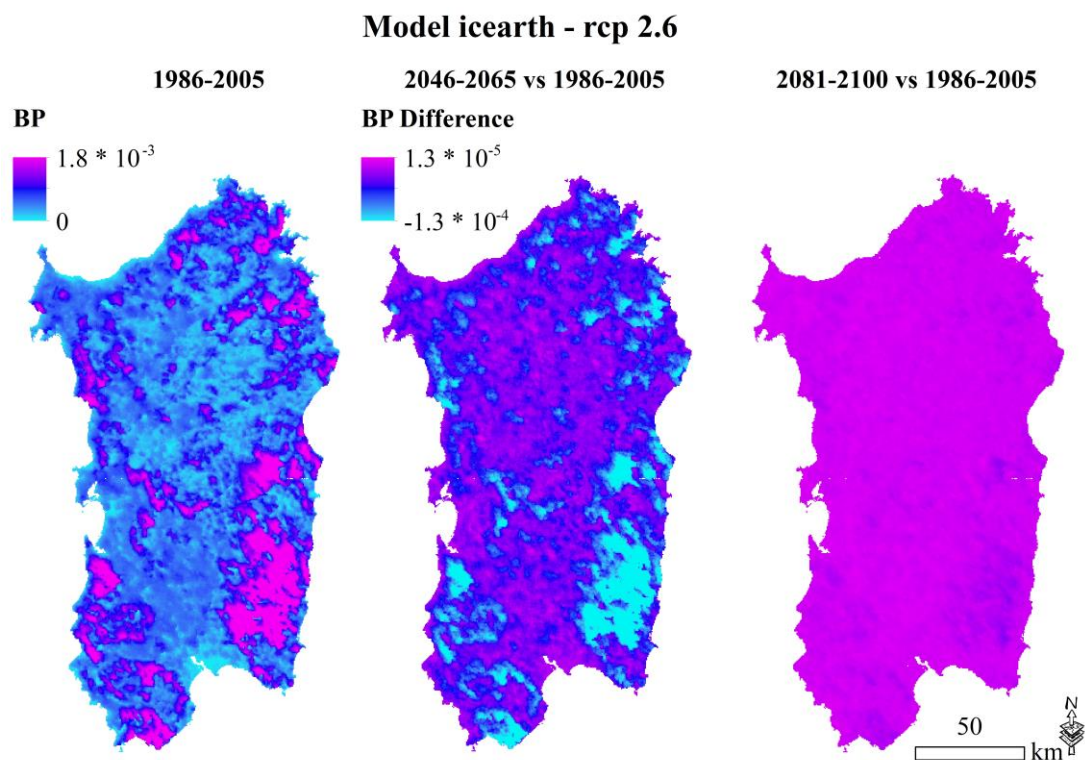

Figure 6 Maps of burn probability (BP) for Sardinia island for the baseline period (1986–2005); difference between near future period (2046-2065) and baseline and between distant future period (2081–2100) and baseline, RCP2.6, Icearth climate model

3.2.1 Baseline 1986-2005

Sardinia island

Using the icearth model, the highest values of **BP** were observed in Sud Sardegna (0.0005) while the lowest values were observed in Oristano and Sassari (0.0003). For the mohc model the highest values of BP were observed in Sud Sardegna (0.0005) while the lowest values were observed in the rest of island (0.0004). For the mpi model the highest values of BP were observed in Sud Sardegna (0.0005) while the lowest values were observed in Cagliari, Oristano and Sassari (0.0003).

Considering **CFL** and the icearth model the highest values were observed in Sud Sardegna (1.16 m) while the lowest values were observed in Oristano (0.74 m). For the mohc model the highest values of CFL were observed in Sud Sardegna (1.24 m) while the lowest values were observed in Oristano (0.80 m). For the mpi model the highest values of CFL were observed in Sud Sardegna (1.14 m) while the lowest values were observed in Oristano (0.73 m).

Regarding **FS** and the icearth model the highest values were observed in Sud Sardegna (1100 ha) while the lowest values were observed in Cagliari (619 ha). For the mohc model the highest values of FS were observed in Sud Sardegna (1221 ha) while the lowest values were observed in Cagliari (671 ha). For the mpi model the highest values of FS were observed in Sud Sardegna (1060 ha) while the lowest values were observed in Cagliari (599 ha).

Corse island

For the icearth model the highest values of **BP** were observed in Corse du Sud (0.0010) while the lowest values were observed in Haute Corse (0.0008). For the mohc model the highest values of BP were observed in Corse du Sud (0.0011) while the lowest values were observed in Haute Corse (0.0010). For the mpi model the highest values of BP were observed in Corse du Sud (0.0009) while the lowest values were observed in Haute Corse (0.0008).

Regarding **CFL** and the icearth model, the highest values were observed in Haute Corse (1.16 m) while the lowest values were observed in Corse du Sud (1.13 m). For the mohc model the highest values of CFL were observed in Haute Corse (1.27 m) while the lowest values were observed in Corse du Sud (1.25 m). For the mpi model the highest values of CFL were observed in Haute Corse (1.13 m) while the lowest values were observed in Corse du Sud (1.10 m).

Considering **FS** for the icearth model, the highest values were observed in Corse du Sud (824 ha) while the lowest values were observed in Haute Corse (677 ha). For the mohc model the highest values of BP were observed in Corse du Sud (988 ha) while the lowest values were observed in Haute Corse (796 ha). For the mpi model the highest values of BP

were observed in Corse du Sud (789 ha) while the lowest values were observed in Haute Corse (649 ha).

Crete island

For the icearth model the highest values of **BP** were observed in Lasithi and Retymno (0.0020) while the lowest values were observed in Chania and Heraklion (0.0017). For the mohc an mpi models the highest values of BP were observed in Lasithi (0.0020) while the lowest values were observed in Chania and Heraklion (0.0017).

Regarding **CFL**, for the icearth, mohc and mpi model the highest values were observed in Lasithi (1.44-1.45 m) while the lowest values were observed in Heraklion (0.89).

Concerning **FS,** for the icearth models the highest values of BP were observed in Lasithi (1774 ha) while the lowest values were observed in Chania (1378 ha). For the mohc models the highest values of BP were observed in Lasithi (1782 ha) while the lowest values were observed in Chania (1381 ha). For the mpi models the highest values of BP were observed in Lasithi (1784 ha) while the lowest values were observed in Chania (1383 ha).

Figure 7 Nomenclature of territorial units for statistics at level 3, NUTS3 of study areas.

3.2.2 RCP 2.6

Under RCP2.6, the values of BP with respect to the baseline in Sardinia and Corsica decreased to a slightly higher extent in the Near Future, whereas in the Distant Future the variation was minor, using the icearth model. The opposite pattern was observed using the moch model, whereas a general increase was predicted using the mpi model. Crete' administrative regions showed the highest increases for BP using the mpi and moch models for both the near and distant future (Table 5).

A similar pattern was observed for the CFL values. In Sardinia an increase with respect to the baseline was detected in the distant future period using the icearth and mpi models.

CFL strongly increased in Crete, especially in the near future using the moch and mpi models. Similar values were simulated for both Corse du Sud and Haute Corse (Table 6).

Finally, FS decrease in all NUT03 in the three islands using the icearth model and for the near future period. Using the other models, it seems that the difference with the respect to the baseline decrease towards the end of the century (Table 7).

Table 5 Percentage (%) changes in BP, icearth, moch, and mpi models under RCP 2.6

	icearth		moch		mpi	
	Near future	Distant future	Near future	Distant future	Near future	Distant future
Sassari	-4	0	5	-1	4	4
Nuoro	-5	-1	4	-2	3	4
Oristano	-4	0	6	-1	5	4
Cagliari	-5	-1	3	-2	3	4
Sud Sardegna	-5	-1	4	-2	4	4
Haute Corse	-2	-1	3	-4	6	8
Corse du Sud	-2	0	4	-4	7	9
Chania	-1	2	9	8	12	10
Heraklion	-1	3	11	9	15	15
Lasithi	-2	1	9	7	12	10
Rethymno	-2	1	9	7	12	10

Table 6 Percentage (%) changes in CFL, icearth, moch, and mpi models under RCP 2.6

	icearth		moch		mpi	
	Near future	Distant future	Near future	Distant future	Near future	Distant future
Sassari	-3	0	4	-1	3	2
Nuoro	-3	0	3	-1	2	2
Oristano	-3	0	4	0	3	2
Cagliari	-3	0	3	-1	2	2
Sud Sardegna	-3	0	3	-1	2	2
Haute Corse	-1	0	2	-2	3	4
Corse du Sud	-1	0	2	-2	4	4
Chania	-1	1	8	7	8	5
Heraklion	-1	2	9	8	10	8
Lasithi	-1	1	7	6	8	5
Rethymno	-1	1	7	6	9	5

Table 7 Percentage (%) changes in FS, icearth, moch, and mpi models under RCP 2.6

	icearth		moch		mpi	
	Near future	Distant future	Near future	Distant future	Near future	Distant future
Sassari	-5	0	6	-1	5	5
Nuoro	-5	-1	6	-1	4	5
Oristano	-4	0	7	0	5	5
Cagliari	-5	-1	6	-1	4	4
Sud Sardegna	-6	-1	5	-2	5	5
Haute Corse	-2	-1	4	-4	6	9
Corse du Sud	-2	-1	4	-4	7	10
Chania	-1	2	11	9	13	10
Heraklion	-1	3	12	10	15	15
Lasithi	0	3	11	9	13	10
Rethymno	-1	2	10	9	13	11

3.2.1 RCP 8.5

Under RCP8.5, the increase of BP was much more prominent, ranging from 7% to 30% in Sardinia, from 7% to 35% in Corse, and from 11% to 40% in Crete (Table 8). In particular, in the distant future period, Heraklion administrative unit showed the highest increase for BP using the mpi model.

Similarly, CFL values greatly increased with respect to the baseline in the Distant Future, from 15% to 22% in Sardinia, from 13% to 19% in Corse, and from 14% to 25% in Crete, whereas in the Near Future the variation was minor (Table 9).

The evolution of FS is similar to BP and CFL, strongly increasing in the distant future in all the sub-areas and using all climate models.

Table 8 Percentage (%) changes in BP, icearth, moch, and mpi models under RCP 8.5

	icearth		moch		mpi	
	Near future	Distant future	Near future	Distant future	Near future	Distant future
Sassari	10	14	9	23	12	28
Nuoro	10	23	8	21	11	26
Oristano	11	26	11	25	13	30
Cagliari	9	21	7	19	10	24
Sud Sardegna	11	25	8	23	12	28
Haute Corse	13	27	7	20	11	30
Corse du Sud	15	31	8	24	13	35
Chania	11	22	15	25	14	28
Heraklion	16	31	19	34	20	40
Lasithi	11	22	14	25	14	29
Rethymno	11	22	14	25	15	30

Table 9 Percentage (%) changes in CFL, icearth, moch, and mpi models under RCP 8.5

	icearth		moch		mpi	
	Near future	Distant future	Near future	Distant future	Near future	Distant future
Sassari	8	18	7	18	8	21
Nuoro	8	17	6	16	7	19
Oristano	9	19	8	19	9	22
Cagliari	7	16	5	15	7	17
Sud Sardegna	8	17	6	16	8	19
Haute Corse	8	16	4	13	7	18
Corse du Sud	9	18	5	14	7	19
Chania	8	14	11	18	9	18
Heraklion	10	19	14	23	12	25
Lasithi	7	14	10	17	9	18
Rethymno	8	14	11	18	9	19

Table 10 Percentage (%) changes in FS, icearth, moch, and mpi models under RCP 8.5

	icearth		moch		mpi	
	Near future	Distant future	Near future	Distant future	Near future	Distant future
Sassari	12	28	12	27	14	33
Nuoro	12	27	11	26	13	31
Oristano	12	28	12	28	14	34
Cagliari	10	24	10	23	12	28
Sud Sardegna	13	19	11	27	14	34
Haute Corse	15	30	8	22	13	34
Corse du Sud	17	36	9	25	14	39
Chania	13	24	17	29	15	31
Heraklion	17	32	21	36	21	41
Lasithi	13	24	17	29	16	30
Rethymno	13	24	17	29	16	32

4. Conclusions

Using a wildfire spread modeling approach, three climate models and two RCP scenarios, here we extend our understanding of the potential impact of future climate change on wildfire for three islands of the Mediterranean.

According to the analysis of the FFMC and DC codes, it seems that the "extreme" fuel moisture categories strongly vary among subareas (NUT3). The most relevant variations in FFMC and DC were observed in the distant future period under RCP8.5 scenario across all climate models, and the increase in the frequency of the driest days suggests that the fire seasons will be longer than the baseline period.

Variability in FFMC and DC codes strongly influences fire characteristics: overall under the RCP2.6 BP, CFL, and FS seem closer to the present conditions towards the end of the century especially in Sardinia and Corsica. On the other hand, under the RCP8.4 the increase is much more prominent, ranging from 7% to 41%, according with fire characteristic and climate models.

The projected results thus suggest an increasing vulnerability of ecosystems and anthropogenic assets to larger fire that could lead to greater losses and escalating

firefighting costs. In addition, the projected increase in wildfire risk is likely to lead to a significant increase in atmospheric emissions. This aspect not only contributes to global warming but has also an important impact on local and regional air quality and eventually implications for human health.

Thus, the information concerning burn probability and intensity maps, obtained through the approach described in this report, can contribute to (i) map fire behaviour changes due to climate change, and to (ii) support fire managers, decision and policy-makers to respond to the potential increase on fire vulnerability and risk, thus contributing to long-term low-carbon transition. Here below we include possible recommendations to incentivize EU islands decarbonization, strengthening science-policy interface, increase social awareness, and contributing to the competitiveness of the European tourism industry.

- Advance in analysing, quantifying and mapping fire behaviour, hazard, risk, and exposure to identify vulnerable areas and to better address mitigation, adaptation and planning policies;
- Identify people and properties at higher risk and enforce protection and self-protection;
- Raise awareness, education and consciousness of the fire-related risks through training and educational campaigns on fire propagation and potential risks, and on what measures we need to apply to reduce behaviours or actions potentially dangerous;
- Develop guidelines to build a "firewise" community, developing strategies and urban plans to minimize risk and losses;
- Foster active forest management to mitigate risk;
- Reduce landscape susceptibility to wildland fires while maintaining ecological diversity through dead and live fuel removal, weed and flammable shrub control, and creation of fuel discontinuity in strategic areas (including wildland-urban interface, very common in touristic areas.

5. References

Anderson HE. Aids to Determining Fuel Models for Estimating Fire Behavior. Ogden, UT: USDA Forest Service, Intermountain Forest and Range Experiment Station, 1982. Report No.: General Technical Report INT-122.

Arca B, Bacciu V, Pellizzaro G, Salis M, Ventura A, Duce P, Brundu G. Fuel model mapping by Ikonos imagery to support spatially explicit fire simulators. In 7th International Workshop on Advances in Remote Sensing andGIS Applications in Forest Fire Management towards an Operational Use of Remote Sensing in Forest Fire Management. Matera, 2009

Arianoutsou M, Kaoukis C, Kazanis D. Fires in the cool coniferous ecosystems of Greece: a random event or an effect of climate change? In: Book of abstracts of the 4th Conference of the Hellenic Ecological Society p 215 (in Greek), 2008

Bedia J, Herrera S, Camia A, Moreno J, Gutiérrez J. Forest fire danger projections in the Mediterranean using ENSEMBLES regional climate change scenarios Clim Change 122:185–199 doi:101007/s10584-013-1005-z, 2014

Dimitrakopoulos A P, Bemmerzouk A M, and Mitsopoulos ID. Evaluation of the Canadian fire weather index system in an eastern Mediterranean environment, Met. Apps, 18, 83–93, doi:10.1002/met.214, 2011

FAO. State of Mediterranean Forests 2013. Food and Agriculture Organization of the United Nations, 2013

Fernandes P. Luz A. Loureiro C. Changes in wildfire severity from maritime pine woodland to contiguous forest types in the mountains of northwestern Portugal For Ecol Manage 260 pp 883-892, 2010

Finney MA. An overview of flammap fire modeling capabilities. Pp. 213–220 in Andrews PL, Butler BW (eds). Fuel Management—How to Measure Success: Conference Proceedings. 28–30 March. Portland, OR: USDA Forest Service, Rocky Mountain Research Station, RMRS-P-41, 2006.

Finney MA. Fire growth using minimum travel time methods. Canadian Journal of Forest Research 32(8):1420–1424, 2002

Giannakopoulos C., LeSager P., Moriondo M., Bindi M., Karali A., Hatzaki M., and Kostopoulou E. Comparison of fire danger indices in the Mediterranean for present day conditions, iForest, 5, 197–203, 2012

Haas JR, Calkin DE, Thompson MP. A national approach for integrating wildfire simulation modeling into wildland urban interface risk assessments within the United States. Landscape and Urban Planning, 2013; 119:44–53.

INFC. Secondo Inventario Nazionale Delle Foreste E Dei Serbatoi Forestali Di Carbonio. Ministero delle Politiche Agricole Alimentari e Forestali, Ispettorato Generale – Corpo Forestale dello Stato; CRA – Istituto Sperimentale per l'Assestamento Forestale e per l'Alpicoltura, 2005

IPCC. Climate Change 2014: Impacts, Adaptation, and Vulnerability. Part B: Regional Aspects. Cambridge, UK and New York, NY, USA: Intergovernmental Panel on Climate Change, Cambridge University Press, 2014. Report No.: Fifth Assessment Report.

Karali A., Hatzaki M., Giannakopoulos C., Roussos A., Xanthopoulos G., and Tenentes V. Sensitivity and evaluation of current fire risk and future projections due to climate

change: the case study of Greece, Nat. Hazards Earth Syst. Sci., 14, 143-153, https://doi.org/10.5194/nhess-14-143-2014, 2014

Koutsias N, Allgöwer B, Kalabokidis K, Mallinis G, Balatsos P, Goldammer JG. Fire occurrence zoning from local to global scale in the European Mediterranean basin: implications for multi-scale fire management and policy iForest 9: 195-204 – doi: 103832/ifor1513-008, 2015

Koutsias N, Arianoutsou M, Kallimanis AS, Mallinis G, Halley JM, Dimopoulos P. Where did the fires burn in Peloponnisos Greece the summer of 2007? Evidence for a synergy of fuel and weather. Agricultural and Forest Meteorology 156: 41-53, 2012

Lavalle C, Micale F, Durrant Houston T, Camia A, Hiederer R, et al. Climate change in Europe 3: Impact on agriculture and forestry. A review. Agronomy for Sustainable Development Springer Verlag/EDP Sciences/INRA 2009 29 (3) ff101051/agro/2008068ff ffhal-00886525

Lozano OM, Salis M, Ager AA, Arca B, Alcasena FJ, Monteiro AT, Finney MA, Del Giudice L, Scoccimarro E, Spano D. Assessing Climate Change Impacts on Wildfire Exposure in Mediterranean Areas. Risk Analysis doi:101111/risa12739, 2016

Marques S, Borges JG, Garcia-Gonzalo J, Moreira F, Carreiras JMB, Oliveira MM, Cantarinha A, Botequim B. Characterization of wildfires in Portugal Eur J For Res 130:775-784, 2011

Moreira F, Viedma O, Arianoutsou M, Curt T, Koutsias N, Rigolot E, Barbati A, Corona P, Vaz P, Xanthopoulos G, Mouillot F, Bilgili E. Landscape –wildfire interactions in southern Europe: implications for landscape management J Environ Manage 92: 2389–2402, 2011

Rothermel's equation (1972) Rothermel RC. A Mathematical Model for Predicting Fire Spread in Wildland Fuels. Ogden, UT: USDA Forest Service, Intermountain Forest and Range Experiment Station, 1972. Report No.: Research paper INT-115

Salis M, Ager AA, Arca B, Finney MA, Bacciu V. Assessing exposure to human and ecological values in Sardinia, Italy. International Journal ofWildland Fire, 2013; 22:549–565.

Scott JH, Burgan RE. Standard Fire Behavior Fuel Models: A Comprehensive Set for Use with Rothermel's Surface Fire Spread Model. Fort Collins, CO: USDA Forest Service, RockyMountain Research Station. Report No.: General Technical Report RMRS-GTR-153, 2005

Scott JH, Reinhardt ED. Assessing Crown Fire Potential by Linking Models of Surface and Crown Fire Behavior. Fort Collins, CO: USDA Forest Service Rocky Mountain Research Station. Report No.: Research paper RMRSRP- 29, 2011

Spano D, Camia A, Bacciu V, Masala F, Duguy B, Trigo R, et al. Recent trends in forest fires in Mediterranean areas and associated changes in fire regimes. In: Moreno J editor Forest

fires under climate social and economic changes in Europe the Mediterranean and other fire–affected areas of the world. FUME Lesson learned and outlook p 6–7, 2014

Turco M, Bedia J, Di Liberto F, Fiorucci P, von Hardenberg J, Koutsias N, et al. Decreasing Fires in Mediterranean Europe. PLoS ONE 11(3): e0150663 doi:101371/journalpone0150663, 2016

Urbieta I R, Zavala G, Bedia J, Gutiérrez J M, Miguel-Ayanz J S, Andrea C, Keeley J E, and Moreno J M. Fire activity as a function of fire–weather seasonal severity and antecedent climate across spatial scales in southern Europe and Pacific western USA. Environ Res Lett 10 114013, 2015

van Wagner CE. Development and Structure of the Canadian Forest Fire Weather Index System. Ottawa: Canadian Forestry Service, Petawawa National Forestry Institute, 1987. Report No.: Forestry Technical Report 35.

Viedma O, Moity N, Moreno JM. Changes in landscape fire-hazard during the second half of the 20th century: Agriculture abandonment and the changing role of driving actors. Agriculture Ecosystems & Environment 207:126–140 doi: 101016/jagee201504011, 2015

Viegas D. X., Bovio G., Ferreira A., Nosenzo A., and Sol B. Comparative study of various methods of fire danger evaluation in southern Europe, Int. J. Wildland Fire, 9, 235–246, 1999
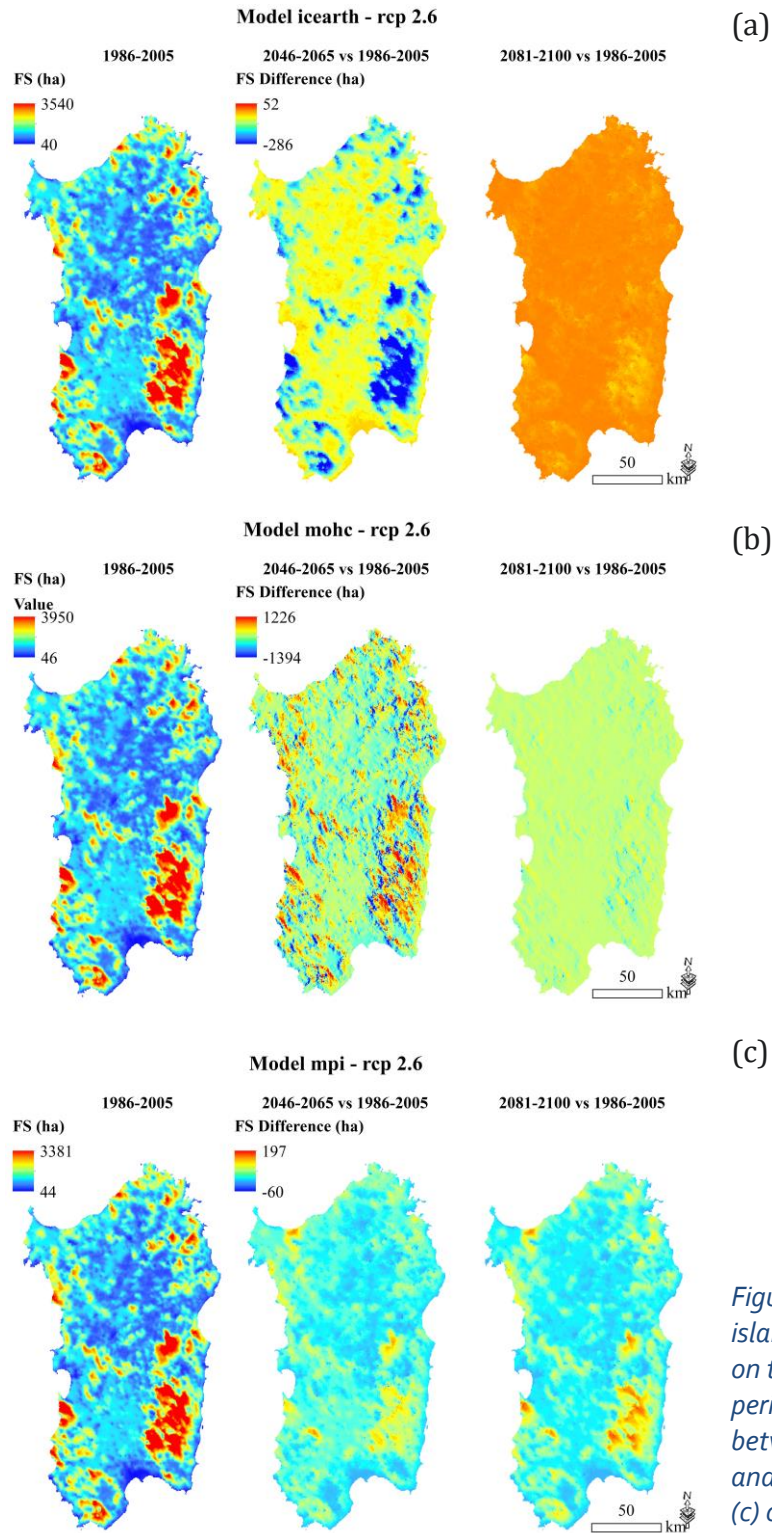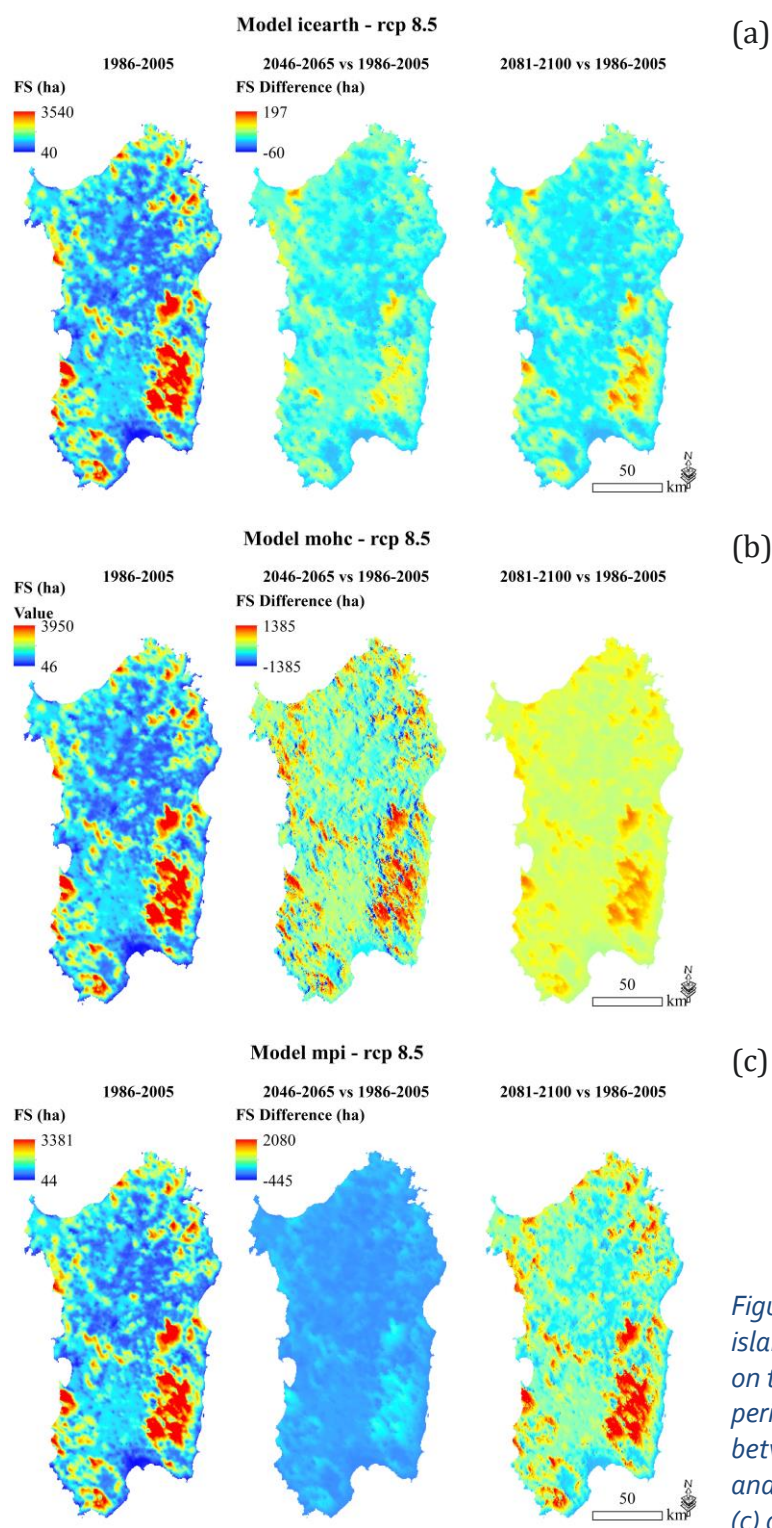
6. ANNEX 1

Figure 8 Maps of Fire Size (FS) for Sardinia island for the baseline period (1986–2005) on the left; difference between near future period (2046-2065) and baseline and between distant future period (2081–2100) and baseline for Icearth (a), moch (b), mpi (c) climate models under RCP2.6
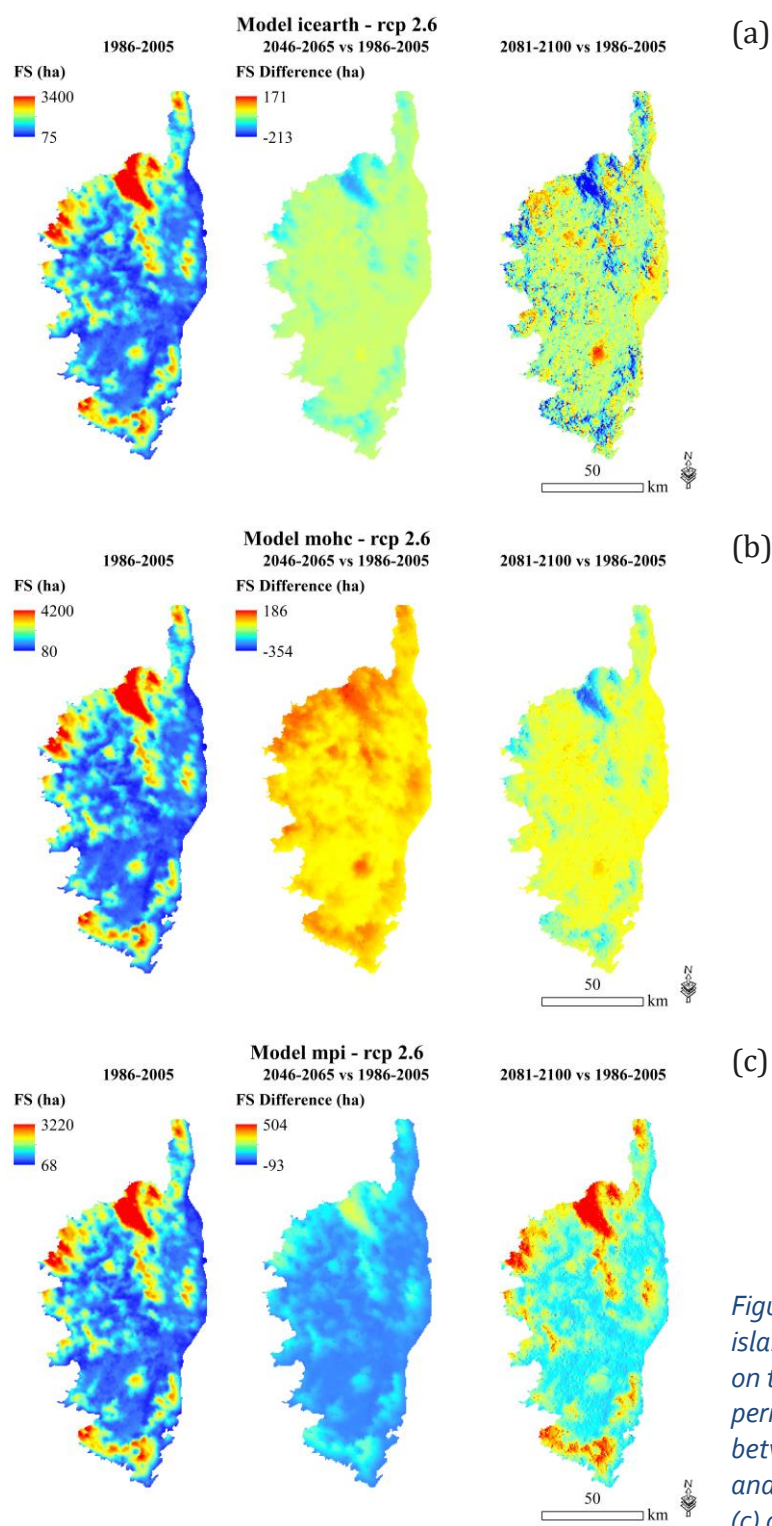
Model icearth - rcp 8.5 (a)

1986-2005   2046-2065 vs 1986-2005   2081-2100 vs 1986-2005

FS (ha)   FS Difference (ha)

3540   197
40   -60

Model mohc - rcp 8.5 (b)

1986-2005   2046-2065 vs 1986-2005   2081-2100 vs 1986-2005

FS (ha)   FS Difference (ha)
Value

3950   1385
46   -1385

Model mpi - rcp 8.5 (c)

1986-2005   2046-2065 vs 1986-2005   2081-2100 vs 1986-2005

FS (ha)   FS Difference (ha)

3381   2080
44   -445

Figure 9 Maps of Fire Size (FS) for Sardinia island for the baseline period (1986–2005) on the left; difference between near future period (2046-2065) and baseline and between distant future period (2081–2100) and baseline for Icearth (a), moch (b), mpi (c) climate models under RCP8.5
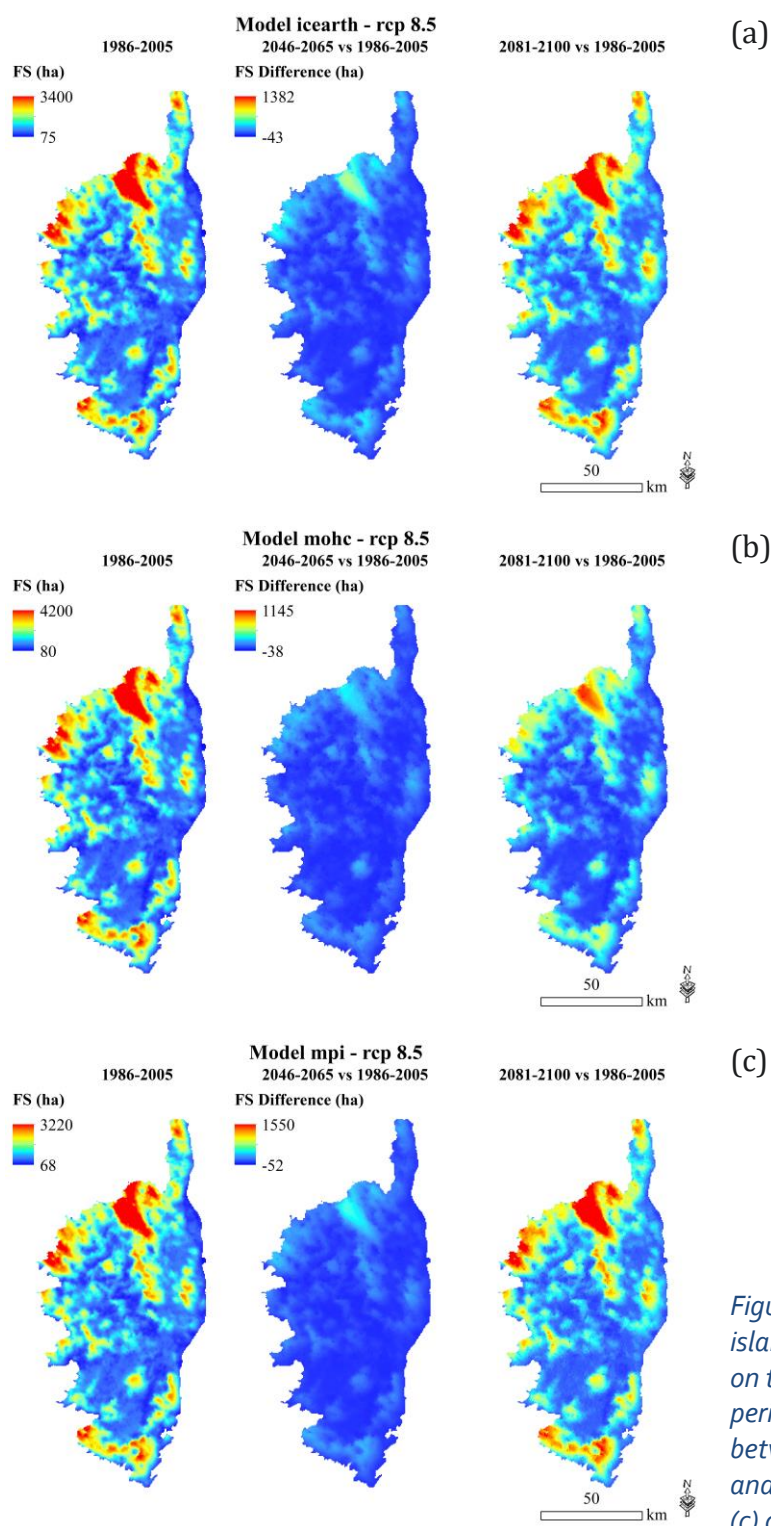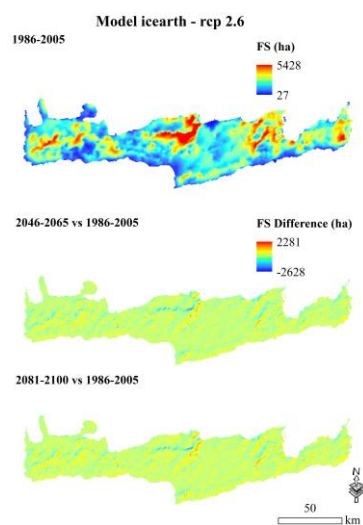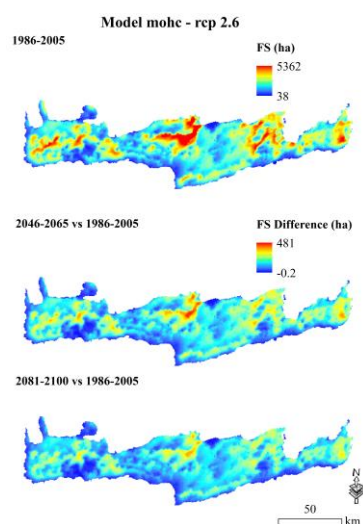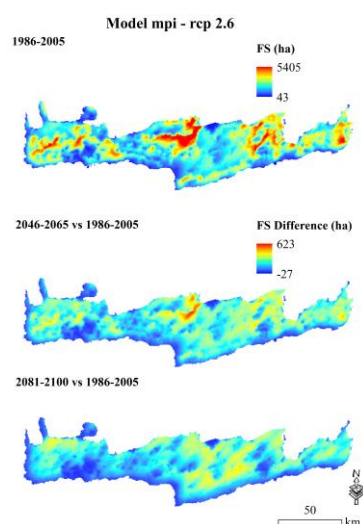
34

Figure 10 Maps of Fire Size (FS) for Corse island for the baseline period (1986–2005) on the left; difference between near future period (2046-2065) and baseline and between distant future period (2081–2100) and baseline for Icearth (a), moch (b), mpi (c) climate models under RCP2.6

Figure 11 Maps of Fire Size (FS) for Corse island for the baseline period (1986–2005) on the left; difference between near future period (2046-2065) and baseline and between distant future period (2081–2100) and baseline for Icearth (a), moch (b), mpi (c) climate models under RCP8.5
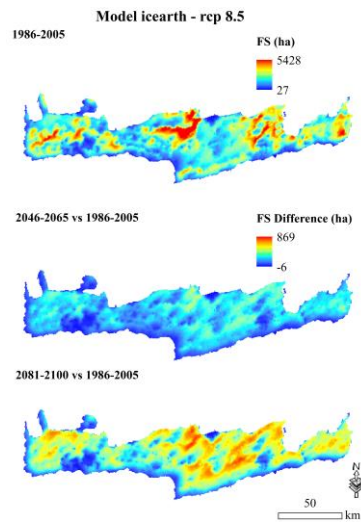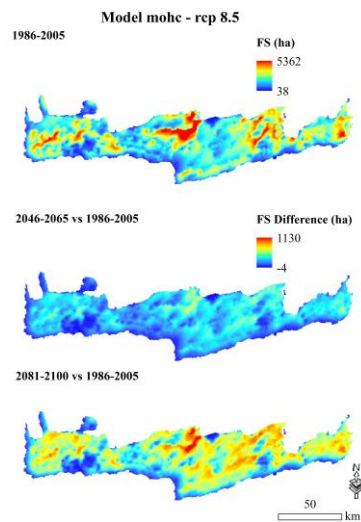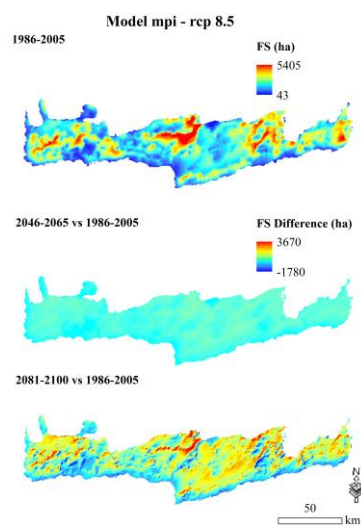
(a)

(b)

(c)

Figure 12 Maps of Fire Size (FS) for Crete island for the baseline period (1986–2005) on the top of the panels; difference between near future period (2046-2065) and baseline and between distant future period (2081–2100) and baseline for Icearth (a), moch (b), mpi (c) climate models under RCP2.6

(a)

(b)

(c)

Figure 13 Maps of Fire Size (FS) for Crete island for the baseline period (1986–2005) on the top of the panels; difference between near future period (2046-2065) and baseline and between distant future period (2081–2100) and baseline for Icearth (a), moch (b), mpi (c) climate models under RCP8.5